Abstract 243

Tumor Area and Microscopic Extent of Invasion to Estimate Circulating Tumor DNA Fraction in Plasma and Detectability of Colorectal Cancer

ASCO GI 2020
January 23-25, 2020
San Francisco, CA

Joerg Bredno, PhD; Jafi A. Lipson, MD; Oliver Venn, DPhil; Samuel Gross, PhD; Alexander P. Fields, PhD; John F. Beausang, PhD; Qinwen Liu, PhD; Jacqueline D. Brooks; Xiaoji Chen, PhD; Margarita Lopatin; Hai Liu, PhD; Nan Zhang, PhD; Lori Zhang; Tony Wu; Brian Allen; Anne-Renee Hartman, MD*; Earl Hubbell, PhD; Arash Jamshidi, PhD; Alexander M. Aravanis, MD, PhD

GRAIL, Inc., Menlo Park, CA

*Employee of GRAIL at the time of this research.

BACKGROUND

- The Circulating Cell-free Genome Atlas (CCGA; NCT02889978) study is a prospective, multicenter, observational, case-control study with longitudinal follow-up to support the development of a plasma circulating cell-free DNA (cfDNA)–based multi-cancer early detection test.
- We previously reported that a targeted methylation (TM) assay and machine-learning classifier detected over 20 cancer types, including breast, lung, colon, prostate, cervical, lymphoid, plasma cell neoplasm, ovarian, bladder, gastrointestinal, liver, pancreatic, head and neck, anorectal, uterine, kidney, melanoma, thyroid, myeloid, and sarcoma, with a single fixed false positive rate of <1%, and simultaneously determined tissue of origin with >90% accuracy.[1-3]
- Previously we showed that the fraction of cfDNA fragments from tumor versus normal cells (tumor fraction, TF) was a stronger predictor of cancer detection than clinical stage and was an equivalent predictor of survival.[4]
- Here, we used colorectal cancer (CRC) as one example to understand the biophysical determinants of TF in solid tumors.
- The model included tumor surface area (TSA) to represent the number of tumor cells and microinvasion beyond the subserosa to represent bloodstream access for DNA fragments.

METHODS

- Blood samples were prospectively collected from participants with newly diagnosed untreated cancer and from participants without a diagnosis of cancer (Figure 1A).
- Specimens in the first CCGA substudy were subjected to a prototype whole-genome bisulfite sequencing (WGBS) assay with a machine-learning classifier that predicted cancer or non-cancer. Samples in the second CCGA substudy were subjected to a TM assay with a newly trained machine-learning classifier that predicted cancer or non-cancer, with tissue of origin predicted for samples with cancer signal detected.[1-3]
- Tumor fraction was determined by comparing variants detected in a targeted sequencing assay of cfDNA from these participants to variants from a whole-genome sequencing (WGS) assay of matched, macrodissected formalin-fixed, paraffin-embedded tumor samples, while using a white blood cell WGS assay to control for germline variants.[4]
- To predict tumor fraction for non-metastatic colorectal adenocarcinomas, we constructed a simple physical model (TF = m * TSA) that assumes a linear relationship (slope, m) with tumor surface area (TSA) and interacts with microinvasion beyond or below the subserosa.
- The model was fit to 27 CRC participants (7 stage I, 11 stage II, and 9 stage III) from the first discovery substudy and was used to predict on 40 CRC participants (12 stage I, 15 stage II, and 13 stage III) from the training set from the second substudy with predictor variables available.

Figure 1. Study Design and CONSORT Diagram

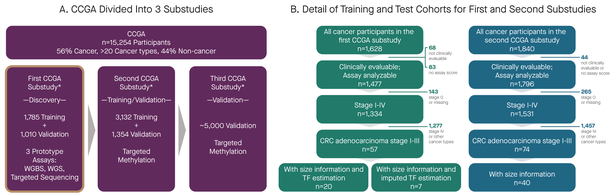

CCGA, Circulating Cell-free Genome Atlas Study; CONSORT, Consolidated Standards of Reporting Trials; CRC, colorectal cancer; TF, tumor fraction; WGBS, whole-genome bisulfite sequencing; WGS, whole-genome sequencing.

**Includes participant samples used in evaluating the classifiers; approximately 2,700 participants not included in evaluating classifiers (eg, used as tissue references or in panel design) not represented.*

RESULTS

- The WGBS classifier detected CRC in 3 of 9 (33%) stage I cases, 11 of 18 (61%) stage II cases, and 17 of 30 (57%) stage III cases.
- The TM classifier detected CRC in 6 of 13 (46%) stage I cases, 16 of 22 (73%) stage II cases, and 29 of 39 (74%) stage III cases.
- TF predicted CRC detection in the first CCGA substudy with an area under the curve of 0.976.
- For the WGBS assay, the classifier score for CRC cases increased approximately linearly with log(TF) before saturation for high tumor fractions (Figure 2).

Figure 2. Detection of Cancer Increases With Increasing TF

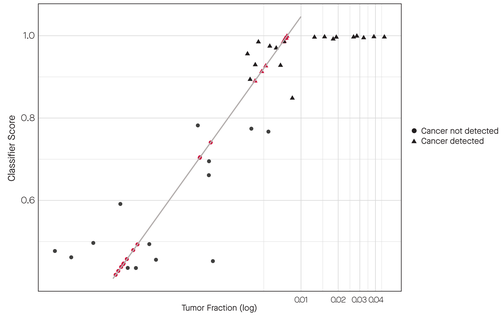

The WGBS prototype assay and classifier showed an increase of classifier scores with the log of TF and saturation around a TF of 0.01. Consequently, for modeling purposes, TF could be imputed from WGBS prototype classifier results with low-to-intermediate TF (red dots).

- TF distributions overlapped for clinical stages I, II, and III (Figure 3A), while TF distributions were clearly separated by microscopic tumor extension (pathological T stage) alone (Figure 3B).

Figure 3. TF Distribution by Clinical Stage (A) and Extent of Microinvasion (B)

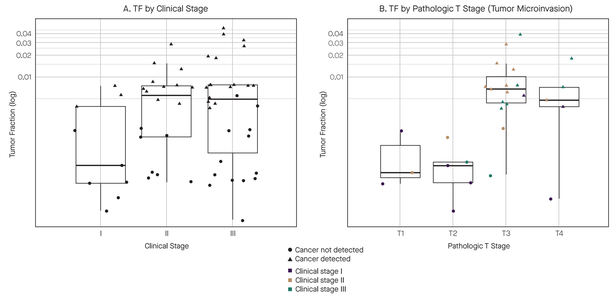

A. TF by clinical stage. Median TF is similar for stages II and III, and distributions widely overlap for stages I-III. B. TF by pathologic T stage (tumor microinvasion). Microscopic tumor extent alone separates cases with high and low TF better than clinical stage. TF, tumor fraction.

- Within a given extent of microinvasion (shallow or deep), TF can be modeled to increase linearly with TSA (Figure 4).
  - The model predicted m = $3.81 \times 10^{-6}/mm^2$ for tumors that invaded beyond the subserosa ($p < 0.001$); this was 4.4 times higher than estimates for tumors below the subserosa (m = $0.866 \times 10^{-6}/mm^2$).

Figure 4. TF Model Including Both Tumor Size and Microinvasion in the First CCGA Substudy

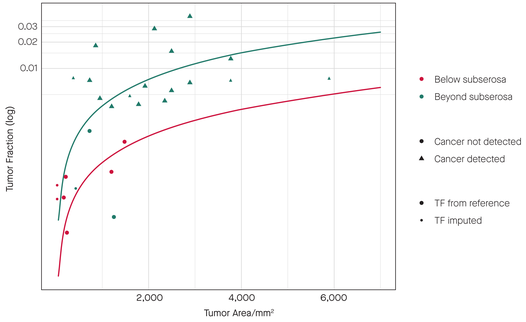

Relationship between tumor area and TF for tumors with microinvasion below the subserosa (red), and tumors that invade beyond the subserosa (teal). The model was fit in linear space and displayed here on a log scale for visualization only. TF increases with tumor area, with slope depending on the depth of microinvasion. TF, tumor fraction.

- The model trained on the WGBS assay predicted CRC detection in the TM assay with an area under the curve of 0.844 (Figure 5).

Figure 5. Receiver Operating Characteristic Curve Based on Model TSA and Microinvasion in the Second CCGA Substudy

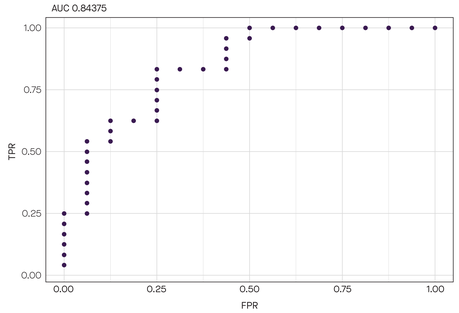

TF estimated by the model using only TSA and microinvasion predicts detection of CRC in the second substudy using the TM assay. AUC, area under the curve; CRC, colorectal cancer; FPR, false positive rate; TF, tumor fraction; TPR, true positive rate for the prediction of cancer detection from cfDNA; TSA, tumor surface area.

CONCLUSIONS

- Higher cfDNA TF was significantly associated with cancer detection.
- The strong relationship between cfDNA WGBS classifier scores and TF in the first substudy implies that TF might be imputed by training a classifier on cfDNA assay results.
- A model using TSA (number of tumor cells) and microinvasion (bloodstream access) predicted TF.
- Tumors not penetrating the subserosa had low cfDNA shedding into the bloodstream that likely limited detection.
- As a greater extent of tumor penetration may be associated with higher-risk disease, these results suggest that the classifier may preferentially detect higher-risk cancers.
- Careful examination of pathologic features of CRC suggest that size (TSA for CRC) and access to circulation (microinvasion for CRC) of solid tumors may strongly affect the shedding of cfDNA into the blood.

References

1. Liu MC, et al. ASCO 2018. Abstract 536.
2. Oxnard GR, et al. ASCO Breakthrough Meeting 2019; Abstract 44.
3. Oxnard GR, et al. ESMO 2019. Abstract 5639.
4. Venn O, et al. Cold Spring Harbor Laboratory Meeting: The Biology of Genomes; May 7 - 11, 2019; Cold Spring Harbor, NY.

Disclosures

All authors are or were employees of GRAIL at the time of this research and hold equity in the company. JB holds equity in Roche. AJ holds equity in Illumina. AMA is an advisor to and holds equity in Foresite Labs.

Copies of this poster obtained through Quick Response (QR) Code are for personal use only and may not be reproduced without permission from ASCO® and the author of this poster.

Corresponding author: aaravanis@grailbio.com

©GRAIL, Inc., 2020. GRAIL is a registered trademark of GRAIL, Inc. All rights reserved.